BENJAMIN-FEIR INSTABILITY OF WAVE PACKETS AT INTERFACE OF LIQUID HALF-SPACE AND LAYER

OLGA AVRAMENKO, VOLODYMYR NARADOVYI

Abstract. The propagation of internal waves in a hydrodynamic system comprising a solid bottom and an upper half-space is investigated. The study is conducted within the framework of a nonlinear low-dimensional model incorporating surface tension on an interface using the method of multi-scale expansions. The evolution equation of the envelope of the wave packet takes the form of the Schrödinger equation. Conditions for the Benjamin-Feir stability of the solution of the evolution equation are identified for various physical and geometrical characteristics of the system. An estimation of the parameter range in which the instability occurs is performed. Significant influence on the modulational stability of the geometrical characteristics of the system and surface tension is observed in each system for relatively small liquid layer thicknesses and waves with a wavelength comparable to the layer thickness.

1. Introduction

The study focuses on examining the modulational instability or Benjamin-Feir instability of wave packets along the interface of liquid layer and half-space above it, considering surface tension. For the first time, modulational instability was presented by Benjamin and Feir [4]. Zakharov continued to investigate this phenomenon and derived the evolution equation for the envelope of the wave packet in the form of a nonlinear Schrödinger equation (NLS) [21]. In subsequent research, more intricate models have been developed. For example, a higher-order NLS equation featuring fifth-order nonlinearity for wave envelopes on a finite-depth fluid surface was derived in [16]. Additionally, the six-wave interaction and classical three-wave equations were formulated from the free surface gravity wave equation incorporating surface tension in [1]. Furthermore, noteworthy contributions include the studies [11] and [7], which provide analytical insights into the role of surface tension in wave propagation on free surfaces and at fluid interfaces.

Here, we review several studies on the propagation of nonlinear waves in layered fluids examined through the framework of multiple-scale expansions. Hasimoto and Ono [10] employed this method to describe a weakly nonlinear solution as a modulated wave packet propagating along a water layer, with its envelope governed by the NLS equation.

2020 *Mathematics Subject Classification.* 76B15, 76B55, 76E99.

Key words and phrases. modulational instability, internal waves, surface tension.

In [13], a detailed analysis of wave packet propagation along the interface of two semi-infinite fluids with surface tension is presented, where the evolution of the envelope is derived as an NLS equation. Grimshaw and Pullin [9] further discussed the stability of finite-amplitude interfacial progressive waves in a two-layer fluid against small perturbations, where an NLS equation is obtained to describe slowly modulated waves using the multiscale expansion. The nonlinear problem of wave-packet propagation along the interface of two semi-infinite fluids is addressed by Selezov et al. [18] using a fourth-order multiple-scale method. We also highlight several studies where the multiscale expansion method has been applied to explore nonlinear wave phenomena in two-component hydrodynamic systems with flows [2, 12, 15]. It is worth noting that the multiple-scale expansion method involves complex transformations, posing challenges as model complexity grows; however, modern computer algebra systems have made it feasible to handle these complexities, which is a central reason for applying this method in the present study.

The following studies investigate the role of the Benjamin-Feir instability within hydrodynamic settings, with a particular focus on its stabilization through dissipation and its impact on extreme wave formation. In [17], it was demonstrated that for waves with a narrow spectral bandwidth and moderate amplitude, specific types of dissipation can stabilize the instability, a finding that was experimentally validated. Direct numerical simulations in [19] further support these results, emphasizing the importance of incorporating dissipation models. Onorato et al. [14] reveal that the Benjamin-Feir index is closely related to modulational instability and the probability of extreme wave events, while [20] and [8] discuss the emergence of nonlinear processes and dispersive shock waves driven by modulation instability. Specifically, Zakharov and Ostrovsky [20] examine nonlinear dynamics arising from modulation instability, whereas El and Hoefer [8] provide a comprehensive review of dispersive hydrodynamics, with a focus on dispersive shock waves. In [3], regimes balancing wind and viscosity effects in wave propagation are identified and validated through experiments. Additionally, spectral methods presented in [6, 5] offer new perspectives on the eigenvalues associated with the Benjamin-Feir instability, detailing stability characteristics in the vicinity of the Stokes wave.

As noted above, although there has been substantial interest in the phenomenon of modulational stability, there remains a lack of comprehensive research on its application to internal wave packets at an interface with surface tension effects.

This article addresses the modulational stability of a two-layer hydrodynamic system, specifically the 'layer with a solid bottom – half-space' (La-HS) configuration, incorporating surface tension through the method of multiscale expansions, carried out using symbolic computation. The accuracy of the results is validated by examining the limiting cases where the layer thickness becomes infinitely large, effectively transitioning to the 'half-space – half-space' (HS-HS) system.

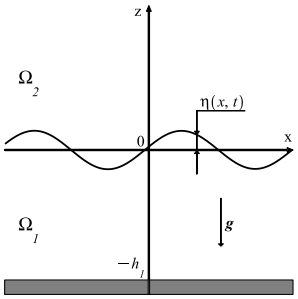

FIGURE 1. Statement of the problem.

2. Problem Statement and Research Method

We examine the propagation of wave packets along the interface $z = \eta(x,t)$ between two incompressible fluid media, Ω_1 and Ω_2, with densities ρ_1 and ρ_2, respectively, taking into account the surface tension T acting on the interface $\eta(x,t)$ (see figure 1). The regions in an undisturbed state have the following form: $\Omega_1 = \{(x,z) : |x| < +\infty, -h_1 < z < 0\}$ and $\Omega_2 = \{(x,z) : |x| < +\infty, 0 < z < +\infty\}$ where the thickness of the layer is h_1.

The mathematical formulation is provided in a dimensionless form, with scaling based on gravitational acceleration g, the density of the lower fluid ρ_1, and a characteristic surface tension T_0. From these parameters, the characteristic length is defined as $L = \left(T_0\rho_1^{-1}g^{-1}\right)^{1/2}$, the characteristic time as $t_0 = \left(Lg^{-1}\right)^{1/2}$, and the characteristic mass as $m_0 = \rho_1 L^3$. Dimensionless quantities, indicated by an asterisk, are defined as follows

$$\begin{gathered} L(x^*, z^*, h_1^*) = (x, z, h_1), \quad \rho_1(\rho_1^*, \rho_2^*) = (\rho_1, \rho_2), \quad t_0 t^* = t, \\ T_0 T^* = T, \quad \alpha L \eta^* = \eta, \quad \alpha L^2 t_0^{-1}(\phi_1^*, \phi_2^*) = (\phi_1, \phi_2). \end{gathered} \tag{2.1}$$

where $\alpha = a/l$ is a small dimensionless parameter representing the wave steepness, with a being the maximum displacement of the interface $\eta(x,t)$ and l the wavelength. It is worth noting that this nondimensionalization approach allows for the exploration of surface tension effects, denoted by T, by setting a fixed characteristic value T_0, in contrast to the method introduced by Nayfeh in [13].

The propagation velocities of the wave packets in the regions Ω_j are defined in terms of the gradients of the potentials $\phi_j(x,z,t)$ for $j = 1, 2$. Consequently, the mathematical formulation of the wave packet propagation problem within this

model takes the form

$$
\begin{gathered}
\Delta\phi_j = 0 \quad \text{in} \quad \Omega_j, \\
\eta_{,t} - \phi_{j,z} = -\alpha\eta_{,x}\phi_{j,x} \quad \text{at} \quad z = \alpha\eta(x,t), \\
\phi_{1,t} - \rho\phi_{2,t} + (1-\rho)\eta + 0.5\alpha\left(\nabla\phi_1\right)^2 - 0.5\alpha\rho\left(\nabla\phi_2\right)^2 \\
-T\left(1+\left(\alpha\eta_{,x}\right)^2\right)^{-1.5}\eta_{,xx} = 0 \quad \text{at} \quad z = \alpha\eta(x,t) \\
\phi_{1,z} = 0 \quad \text{at} \quad z = -h_1, \quad |\nabla\phi_2| \to 0 \quad \text{at} \quad z \to +\infty.
\end{gathered} \tag{2.2}
$$

The surface elevation and velocity potentials in the domains $\Omega_j (j = 1, 2)$ are represented according to the method of multiple scales

$$
\begin{aligned}
\eta(x,t) &= \sum\nolimits_{n=1}^{3} \alpha^{n-1}\eta_n(x_0, x_1, x_2, t_0, t_1, t_2) + \mathrm{O}(\alpha^3), \\
\phi_j(x,z,t) &= \sum\nolimits_{n=1}^{3} \alpha^{n-1}\phi_{jn}(x_0, x_1, x_2, z, t_0, t_1, t_2) + \mathrm{O}(\alpha^3),
\end{aligned} \tag{2.3}
$$

where $x_n = \alpha^n x$, $t_n = \alpha^n t$ are the spatial and temporal scaling variables.

The substitution (2.3) into the problem (2.2) leads to the first three linear approximations with respect to the unknown functions, which are coefficients in the expansion (2.3). Here are the solutions for the first approximation

$$\eta_1 = A\exp(\mathrm{i}\theta) + \overline{A}\exp(-\mathrm{i}\theta), \tag{2.4}$$

$$\phi_{11} = -\tfrac{\mathrm{i}\omega}{k\sinh(kh_1)}\left(A\exp(\mathrm{i}\theta) - \overline{A}\exp(-\mathrm{i}\theta)\right)\cosh(k(h_1+z)), \tag{2.5}$$

$$\phi_{21} = \tfrac{\mathrm{i}\omega}{k}\left(A\exp(\mathrm{i}\theta - kz) - \overline{A}\exp(-\mathrm{i}\theta - kz)\right), \tag{2.6}$$

where $A = A(x_1, x_2, t_1, t_2)$ is the envelope of the wave packet, $\overline{A}$ is the complex conjugate of A, k is the wave number, ω is the frequency of the wave packet center, $\theta = kx_0 - \omega t_0$. The dispersion relation is given by

$$\omega^2 = \frac{k - \rho k + Tk^3}{\coth(kh_1) + \rho}. \tag{2.7}$$

Based on these solutions of the first approximation (2.4)-(2.6) and the dispersion relation (2.7), conditions of solvability and solutions of the second approximation are obtained. Below is the analytical expression for $\eta_2(x,t)$

$$\eta_2 = b_0 A\overline{A} + \Lambda A^2\exp(2\mathrm{i}\theta) + \text{c.c.} \tag{2.8}$$

where the coefficients b_0 and Λ have the form

$$
\begin{gathered}
b_0 = -\tfrac{\omega^2}{2(1-\rho)\sinh^2(kh_1)}, \\
\Lambda = \tfrac{k\omega^2\coth(kh_1)\left(2\sinh^2(kh_1)(1-\rho)+3\right)}{2\cosh(2kh_1)\omega^2 - (4Tk^3 + k - \rho - 2\omega^2\rho)\sinh(2kh_1)}.
\end{gathered}
$$

The solvability conditions for the second approximation is in the form

$$W_{11}A_{,t_1} + W_{12}A_{,x_1} = 0, \tag{2.9}$$

where the coefficients W_{11} and W_{12} depend only on the geometric and physical parameters of the system T, ρ, k, and h_2. After transformations, the condition (2.9) can be rewritten as

$$A_{,t_1} + \omega' A_{,x_1} = 0, \tag{2.10}$$

where $\omega' = \mathrm{d}\omega/\mathrm{d}k$ is the group velocity.

For the problem of the third approximation, the solvability condition was found to be

$$W_{21} A_{,t_2} + W_{22} A_{,x_2} + W_{23} A_{,x_1 x_1} + W_{24} A^2 \overline{A} = 0, \tag{2.11}$$

where the coefficients W_{21}, W_{22}, W_{23}, and W_{24} depend only on T, ρ, k, h_2. After analytical transformations, considering the dispersion relation (2.7), equations (2.10) and (2.11), and transitioning from the scaling variables $t_0, t_1, t_2, x_0, x_1, x_2$ to variables x and t, the evolution equation for the envelope of wave packets on the contact surface can be written as

$$\mathrm{i}A_{,t} + \mathrm{i}\omega' A_{,x} + 0.5\omega'' A_{,xx} = -\alpha \omega^{-1} J A^2 \overline{A}, \tag{2.12}$$

here $\omega'' = \mathrm{d}^2\omega/\mathrm{d}k^2$ and

$$J = \frac{W_1 \omega^6 + W_2 \omega^4 + W_3 \omega^2 + W_4}{W_5 \omega^2 + W_6} k,$$

where $W_1 = \cosh(2kh_1)\mathrm{csch}^3(kh_1) + 2\rho\mathrm{csch}(kh_1)\coth(kh_1)$,

$$\begin{aligned}
W_2 = {} & 6k\rho^3 \sinh^2(kh_1)\cosh(kh_1) - 2k\rho^2\big[\cosh(2kh_1)\mathrm{csch}(kh_1) \\
& + 2\cosh(2kh_1)\cosh(kh_1) - 6\sinh(kh_1)\cosh^2(kh_1) + \cosh^3(kh_1) \\
& + \cosh(2kh_1)\cosh(kh_1)\coth(kh_1)\big] + k\rho\big[2\cosh(2kh_1)\mathrm{csch}(kh_1) \\
& + 6\cosh(2kh_1)\cosh(kh_1) + 1.5\coth(kh_1)\mathrm{csch}(kh_1) \\
& - 2\sinh^2(kh_1)\cosh(kh_1) + 2\cosh(2kh_1)\coth(kh_1)\mathrm{csch}(kh_1) \\
& - 12\sinh(kh_1)\cosh^2(kh_1) + 2\cosh(2kh_1)\cosh(kh_1)\coth(kh_1)\big] \\
& - k\big[5.5\coth(kh_1)\mathrm{csch}(kh_1) + 2\cosh(2kh_1)\cosh(kh_1)\coth^2(kh_1) \\
& - 6\cosh^2(kh_1)\coth(kh_1)\mathrm{csch}(kh_1) + 2\coth(kh_1)\mathrm{csch}(kh_1)\cosh^4(kh_1)\big] \\
& - 4Tk^3\mathrm{csch}(kh_1)\coth(kh_1),
\end{aligned}$$

$$\begin{aligned}
W_3 = {} & k^2(1-\rho)\Big[(1-\rho)\{2\rho\cosh(kh_1)\sinh^2(kh_1) \\
& + 6\sinh(kh_1)\cosh^2(kh_1) - 2\cosh(kh_1)\cosh(2kh_1)\coth(kh_1)\} \\
& - 1.5Tk^2\mathrm{csch}(kh_1)\cosh(2kh_1) + 11Tk^2\rho\cosh(kh_1)\sinh^2(kh_1) \\
& + 24Tk^2\sinh(kh_1)\cosh^2(kh_1) - 6.5Tk^2\mathrm{csch}(kh_1)\cosh(2kh_1)\cosh^2(kh_1)\Big],
\end{aligned}$$

$$W_4 = Tk^5\big(1-\rho\big)\big[1.5\rho - 1.5 - 6Tk^2\big]\cosh(kh_1)\sinh^2(kh_1),$$
$$W_5 = 2\big(1-\rho\big)\big(\rho\sinh(kh_1)+\cosh(kh_1)\big)\big(\rho\sinh(2kh_1)+\cosh(2kh_1)\big),$$
$$W_6 = k\big(1-\rho\big)\big(\rho - 1 - 4Tk^2\big)\big(\cosh(kh_1)+\rho\sinh(kh_1)\big)\sinh(2kh_1).$$

Transitioning to a moving frame with the group velocity by substituting $\xi = x - \omega' t$ and $\zeta = t$, let's rewrite the envelope equation (2.12) in the form of a NLS

$$\mathrm{i}A_{,\zeta} + 0.5\omega'' A_{,\xi\xi} = -\alpha\omega^{-1}JA^2\overline{A}. \tag{2.13}$$

To derive the modulation stability condition of wave packets, let's consider one of the solutions of the equation (2.13) which depends only on time

$$A = a\exp(\mathrm{i}\alpha a^2\omega^{-1}J\zeta), \tag{2.14}$$

where a is a constant. Substituting (2.14) into (2.4) and (2.8), taking into account the expansion (2.3), and transitioning from variables (ξ,ζ) to (x,t), we obtain

$$\eta(x,t) = 2a\cos(kx-\hat{\omega}t) + 2\alpha\left(b_0 + \Lambda\cos(2kx - 2\hat{\omega}t)\right) + \mathrm{O}(\alpha^2), \tag{2.15}$$

where $\hat{\omega} = \omega - \alpha a^2\omega^{-1}J$. Utilizing the methodology described in [13], based on (2.13), (2.14), and (2.15), we obtain the modulation or Benjamin-Feir stability condition for wave packets in the HS-La model in the form of

$$J\omega'' < 0. \tag{2.16}$$

It's worth noting that condition (2.16) coincides with the condition obtained for the HS-HS model of wave propagation at the interface between two semi-infinite regions, as described in [13]. To confirm the correctness of the analytical results for the La-HS system, a limiting transition to the HS-HS system was performed as $h_1 \to -\infty$. All equations and expressions for Λ and J degenerate into the corresponding equations and expressions previously derived in [13] for the HS-HS system. This confirms the correctness of the obtained analytical results.

3. Modulational stability analysis

In this section, a description and analysis of stability diagrams on the (ρ, k) plane for La-HS system is presented. Each stability diagram is divided into regions of linear instability (dark shading) and linear stability. The region of linear stability, in turn, consists of areas of nonlinear stability (unshaded) and nonlinear instability, or in other words - instability of the envelope of the wave packet, or modulational instability, or Benjamin-Feir instability (light shading).

The condition for linear stability is determined by the same relationship, namely, when the wave numbers are greater than a critical value, $k > k_c = \sqrt{(\rho-1)/T}$, therefore, in all the stability diagrams presented below, the $(\rho,\ k)$ plane is divided by the curve $k = k_c$ (black curve) into a region of linear instability located below this curve, and a region of linear stability located above and to the left of it.

As previously indicated in (2.16), the sign of the expression $J\omega''$ determines whether the envelope of the wave packet is stable or not, i.e., whether modulational

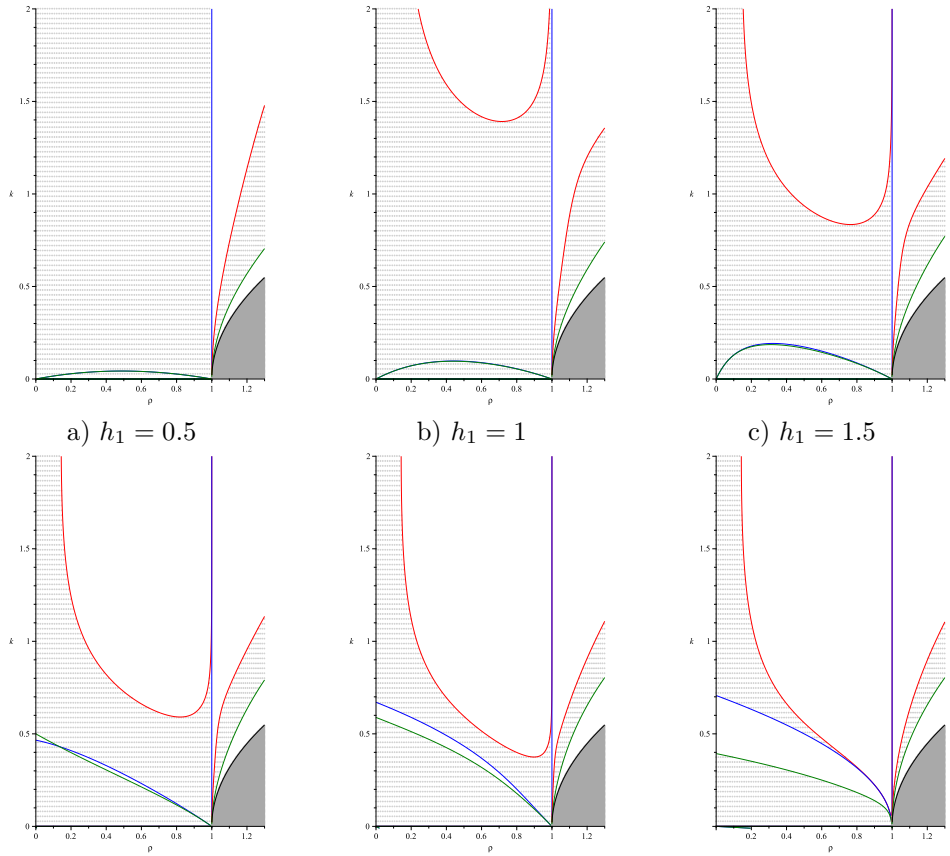

a) $h_1 = 0.5$ b) $h_1 = 1$ c) $h_1 = 1.5$

d) $h_1 = 2$ e) $h_1 = 3$ f) $h_1 = 20$

FIGURE 2. Modulational stability diagram for $T = 1$.

stability exists or not. Thus, the region of linear stability is divided into regions of nonlinear stability and instability by curves along which $J = 0$ (red curves), $J \to \infty$ (blue curves), and $\omega'' = 0$ (green curves).

Below is a description of the regions of modulational stability and instability, which will be referred to as 'stability' and 'instability' regions for brevity in the following discussion.

The stability diagrams at different layer thicknesses and $T = 1$ are presented in figure 2. For all investigated parameter values, there exists a certain similarity in the diagrams in the right part, where the density ratio $\rho > 1$. In this region, the linear instability region lies below the curve $k = k_c$ (black curve), while above it, three alternating regions of nonlinear stability and instability are situated. The

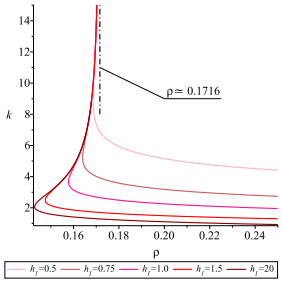

FIGURE 3. The vicinity of the asymptote for $T = 1$

vertical line $\rho = 1$, along which $J \to \infty$, separates the region of nonlinear stability to the right from the region of nonlinear instability to the left.

We can also mention the presence of a region of nonlinear stability with asymptotes $\rho = 1$ and $\rho \simeq 0.1716$ for capillary waves when $\rho < 1$. We will refer to this region as the 'upper' region. For a layer thickness of $h_1 = 0.5$, the 'upper' region of nonlinear stability begins at $k > 2$, which is why it is not visible in figure 2 *a*. As the layer thickness increases to $h_1 = 1, 1.5, 2, 3, 20$ (see figures 2 *b, c, d, e, f*), the 'upper' region descends, and its lower point tends towards $(1, 0)$ as $h_1 \to \infty$.

On figure 3, the region around the asymptote $\rho \simeq 0.1716$ is presented for different values of layer thickness $h_1 = 0.5, 1, 1.5, 2, 3, 20$ at $T = 1$. It's worth noting that we observe the following dependence: the thinner the layer, the further to the right the curve separating the instability region from the 'upper' stability region. The limiting position of these curves as the layer thickness increases $h_1 \to \infty$ remains the same, corresponding to the case of two half-spaces system [13], which is evident at $h_1 = 20$.

In the lower part of the diagram, there is an 'elongated' region, bounded above by a blue curve $J \to \infty$ and below by a green curve $\omega'' = 0$. For small layer thicknesses h_1, it essentially degenerates into a 'cut' on the $(\rho,\ k)$ plane, which is clearly visible for $h_1 = 0.5, 1, 1.5$ (figures 2 *a, b, c*). For these values of layer thickness, the blue curve along which $J \to \infty$ and the green curve where $\omega'' = 0$ almost coincide creating a "cut" on the plane (ρ, k) which starts from the origin and ends at the point $(1, 0)$. As the layer thickness increases, both curves rise above the origin, still not diverging far from each other, having a point of intersection, as seen for $h_1 = 2$ (figure 2 *d*). For even larger thicknesses, the 'elongated' region of nonlinear stability expands, as evident for $h_1 = 3, 20$ (figures 2 *e, f*). As $h_1 \to \infty$, this region completely coincides with the corresponding region of the two liquid half-spaces system [13], and as $h_1 \to \infty$ and $\rho = 0$, it corresponds to [21].

We now present an analysis of the dependence of modulational stability on surface tension. Figures 4 *a, b, c* depict stability diagrams for a layer thickness of $h_1 = 1.5$ with surface tension coefficient values of $T = 0.75, 1.25, 1.75$, while figures 4 *d, e, f* represent diagrams for $h_1 = 1.5$ with the same values of

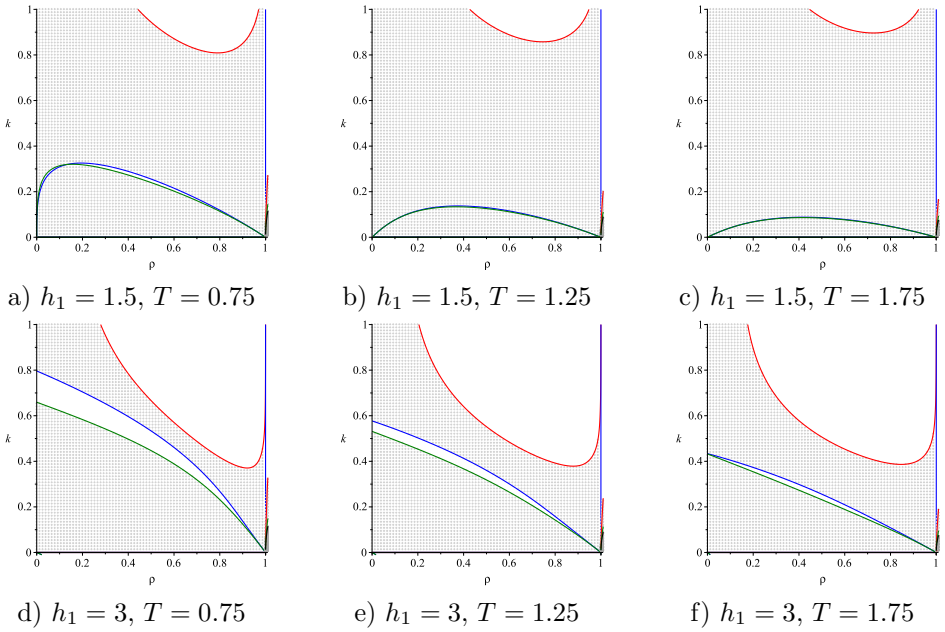

a) $h_1 = 1.5$, $T = 0.75$ b) $h_1 = 1.5$, $T = 1.25$ c) $h_1 = 1.5$, $T = 1.75$

d) $h_1 = 3$, $T = 0.75$ e) $h_1 = 3$, $T = 1.25$ f) $h_1 = 3$, $T = 1.75$

FIGURE 4. Modulational stability diagram of wave packets.

$T = 0.75, 1.25, 1.75$. It can be observed that as the surface tension increases, all regions of the stability diagram undergo significant deformation. As the surface tension increases ($T = 0.75, 1.25, 1.75$) with a layer thickness of $h_1 = 1.5$, the 'cut', which is a degeneration of the 'elongated' region, in the long-wave region diminishes and approaches the horizontal axis, while the 'upper' stability region slightly shifts upward and widens. Furthermore, when the layer thickness is $h_1 = 3$, the 'elongated' stability region significantly narrows as the surface tension increases $T = 0.75, 1.25$, almost turning into a 'cut' in the instability region at $T = 1.75$. Meanwhile, the lower point of the 'upper' stability region slightly rises upward, and the region itself becomes substantially wider.

As noted above in subsection **??**, the low-dimensional models HS-La and La-HS considered in this study can be interpreted as 3D models of wave propagation in two-layer liquid media within a channel.

4. Estimation of the parameter range

Let us now move from the dimensionless variables to the evaluation of actual dimensional quantities. Let the nondimensionalization (2.1) be carried out based on the following values: gravitational acceleration $g = 9.80665$ m/s^2, density of the lower fluid $\rho_1 = 10^3$ kg/m^3, and a characteristic surface tension, for instance, the surface tension on the free surface of water $T_0 = 0.07286$ N/m.

Let us consider the case when the nondimensional thickness of the layer ${h_1}^* = 1$. Upon conversion to dimensional quantities, we have $h_1 = 0.00273$ m. Thus, we have a case of a relatively thin liquid layer, which may occur in laboratory experiments and some technological installations, but is not applicable to the study of waves in the ocean. It is evident that the range of waves, whose lengths are comparable to the thickness of the layer, corresponds to the range of wave numbers from 0.5 to 1.0. In this range, the wave amplitudes do not exceed 15% of the layer thickness. As the wave numbers increase, the wave lengths decrease and become significantly smaller than the layer thickness.

With the considered layer thickness $h_1^* = 1$ and for $T^* = 1$, the 'upper' region of modulational stability arises at $\rho \simeq 0.75$ and $k \simeq 1.41$, corresponding to short waves. As k increases, the 'upper' stability region expands (see figure 2 *b*). During the study, various thicknesses of the layer were also considered at different values of surface tension. In each case, a significant influence of the geometric parameters of the system and the magnitude of the surface tension was noted, particularly for relatively small thicknesses of the liquid layers and waves, as well as for wavelengths comparable to them.

Conclusions

We summarize the key features of modulational stability regions in 2D hydrodynamic system a hydrodynamic system consisting of a solid bottom and an upper half-space on the (ρ, k) plane, examining various layer thicknesses and surface tension values. For cases where $\rho < 1$, two main stability regions are identified: the 'upper' region and the 'elongated' region. Specifically, (i) the 'upper' region occurs at high wavenumbers, spanning a wide range of density ratios, with boundaries at approximately $\rho \simeq 0.1716$ and $\rho = 1$; (ii) the 'elongated' region, under certain parameter conditions, reduces to a narrow 'cut' in the lower part of the stability diagram, nearly vanishing, where wave packet envelopes are unstable across most parameter values for long wavelengths. Our findings highlight the substantial impact of both layer thickness and surface tension on the stability characteristics, especially in the case where the wavelengths are comparable to the layer thickness.

Acknowledgement Dr. Olga Avramenko expresses gratitude to the Research Council of Lithuania for the support in preparing this article.

References

[1] Ablowitz, J., Xu-Dan Luo, Ziad H.: Musslimani Six wave interaction equations in finite-depth gravity waves with surface tension. J. Fluid Mech., 961:A3 (2023); doi: 10.1017/jfm.2023.128

[2] Abrashkin, A. A., Pelinovsky, E. N.: Dynamics of a wave packet on the surface of an inhomogeneously vortical fluid (Lagrangian description). Izv. Atmos. Ocean. Phys. **54**, 101–105 (2018); doi: 10.1134/S0001433818010036

[3] Armaroli, A., Eeltink, D., Brunetti, M., Kasparian, J.: Nonlinear stage of Benjamin-Feir instability in forced/damped deep-water waves. Physics of Fluids **30(1)**, 017102 (2018); doi: 10.1063/1.5006139

[4] Benjamin, T. B., Feir, J. E.: The disintegration of wave trains on deep water Part 1. Theory. Journal of Fluid Mechanics, **27(3)**, 417-430 (1967); doi: 10.1017/S002211206700045X
[5] Berti, M., Maspero, A., Ventura, P.: Benjamin–Feir Instability of Stokes Waves in Finite Depth. Archive for Rational Mechanics and Analysis **247**, 91 (2023); doi: 10.1007/s00205-023-01916-2
[6] Berti, M., Maspero, A., Ventura, P.: Full description of Benjamin-Feir instability of Stokes waves in deep water. Inventiones Mathematicae **230**, 651-711 (2022); doi: 10.1007/s00222-022-01130-z
[7] Düll, W.-P.: Validity of the Nonlinear Schrödinger Approximation for the Two-Dimensional Water Wave Problem with and without Surface Tension in the Arc Length Formulation. Arch. Rational Mech. Anal. **239**, 831–914 (2021); doi: 10.1007/s00205-020-01586-4
[8] El, G. A., Hoefer, M. A.: Dispersive shock waves and modulation theory. Physica D: Nonlinear Phenomena **333**, 11-65 (2016); doi: 10.1016/j.physd.2016.04.006
[9] Grimshaw R. H. J., Pullin D. I.: Stability of finite-amplitude interfacial waves. Part 1. Modulational instability for small-amplitude waves. J. Fluid Mech. **160**, 297-315 (1985); doi: 10.1017/S0022112085003494
[10] Hasimoto H., Ono H.: Nonlinear Modulation of Gravity Waves. Journal of the Physical Society of Japan **33(3)**, 805–811 (1972); doi: 10.1143/JPSJ.33.805
[11] Ionescu, A. D., Pusateri, F.: Global regularity for 2D water waves with surface tension. Mem. Amer. Math. Soc. **256**, 123 pp (2018); doi: 10.1090/MEMO/1227
[12] Li, S., Chen, J., Cao, A., Song, J.: A nonlinear Schrödinger equation for gravity waves slowly modulated by linear shear flow. Chinese Phys. B **28**, 124701 (2019); doi: 10.1088/1674-1056/ab53cf
[13] Nayfeh A.: Nonlinear propagation of wave-packets on fluid interface. Trans. ASME, Ser. E: J. Appl. Mech. **43(4)**, 584-588 (1976); doi: 10.1115/1.3423936
[14] Onorato, M., Osborne, A. R., Serio, M., Cavaleri, L., Brandini, C., Stansberg, C. T.: Extreme waves, modulational instability and second order theory: wave flume experiments on irregular waves. European Journal of Mechanics - B/Fluids **25(5)**, 586-601 (2006); doi: 10.1016/j.euromechflu.2006.01.002
[15] Pal, T., Dhar, A.K.: Weakly nonlinear modulation of interfacial gravity-capillary waves. Ocean Dynamics **74**, 133–147 (2024); doi: 10.1007/s10236-023-01594-4
[16] Sedletsky, Y.: A fifth-order nonlinear Schrödinger equation for waves on the surface of finite-depth fluid. Ukrainian Journal of Physics **66(1)**, 41-54 (2021); doi: 10.15407/ujpe66.1.41
[17] Segur, H. , Henderson, D., Carter, J., Hammack, J., Li, C., Pheiff, D., Socha, K.: Stabilizing the Benjamin–Feir instability. Journal of Fluid Mechanics **539**, 229-271 (2005); doi: 10.1017/S002211200500563X
[18] Selezov I., Avramenko O., Kharif C., Trulsen K.: High-order evolution equation for nonlinear wave-packet propagation with surface tension accounting. Comptes Rendus. Mécanique **331(3)**, 197-201 (2003); doi: 10.1016/S1631-0721(03)00043-3
[19] Wu, G., Liu, Y., Yue, D. K. P.: A note on stabilizing the Benjamin–Feir instability. Journal of Fluid Mechanics **556**, 45-54 (2006); doi: 10.1017/S0022112005008293
[20] Zakharov, V. E., Ostrovsky, L. A.: Modulation instability: The beginning. Physica D: Nonlinear Phenomena **238(5)**, 540-548 (2009); doi: 10.1016/j.physd.2008.12.002
[21] Zakharov, V. E.: Stability of periodic waves of finite amplitude on the surface of a deep fluid. Journal of Applied Mechanics and Technical Physics **9**, 190-194 (1968); doi: 10.1007/BF00913182

Vytautas Magnus University, K. Donelaičio g. 58, Kaunas, 44248, Lithuania
Email address: olga.avramenko@vdu.lt

Volodymyr Vynnychenko Central Ukraine State University, Shevchenko St. 1, Kropyvnytskyi, 25006, Ukraine
Email address: v.v.naradovyi@cuspu.edu.ua